REVERSE-VORTEX PLASMA STABILIZATION: EXPERIMENTS AND NUMERICAL SIMULATION

Alexander Chirokov, Alexander Gutsol, Alexander Fridman and Lawrence Kennedy

University of Illinois at Chicago, Department of Mechanical Engineering
842 West Taylor Street, Chicago, Illinois 60607-7022, USA

Abstract

Recently invented Reverse-Vortex method for plasma stabilization is compared with the traditional Forward-Vortex one. Experimental calorimetric investigations were carried out to compare energetic characteristics of microwave and radio-frequency inductively coupled plasma torches and gas combustion chamber. FLUENT programming package was used for numerical simulations of electrodeless plasma torches. Results of investigations show that Reverse-Vortex stabilization is very promising for different plasma technology applications.

1. Introduction

One of the common methods for plasma-wall insulation used in plasma sources is the vortex flow. Due to buoyancy in the centrifugal force field a hot plasma fluid is fixed on the system axis. In the usual vortex method of plasma stabilization and insulation the vortex generator is placed upstream relatively to the electric discharge and the outlet of the plasma jet is directed to the opposite side, so we named this method as Forward-Vortex Stabilization (FVS). In such systems with intensive flow rotation a central reverse flow forms and transfers heat energy from the center of the vortex-stabilized plasma upstream, and a significant part of this energy is absorbed by the plasma torch walls and becomes lost. To avoid these energy losses and improve characteristics of plasma torches the Reverse-Vortex Stabilization (RVS) was developed [1]. An idea of RVS is to direct an outlet of the plasma jet along the axis to the swirl generator side [1, 2]. In this case the plasma gas comes into discharge zone from all sides except the outlet side and no significant recirculation zone is formed.

From the application point of view, probably the most promising property of the reverse vortex flows is the possibility to inject an additional axial flow from the closed end of the system without substantially disrupting the flow pattern. Therefore, it is possible to insert a new substance (gaseous or disperse) into plasma for treatment in the active zone, and the treated products should not interact with the plasma torch wall significantly. The lack of such properties in discharges with traditional stabilization [3] restricts their applications.

In this paper we present the review of experimental results obtained during investigation of Micro-Wave (MW) [2] and Radio-Frequency (RF) [4] Inductively Coupled Plasma (ICP) torches and gas combustion chamber [5-7], and also the results of numerical simulations of investigated electrodeless plasma torches: MW [7-9] and RF ICP [10] including new results for ICP obtained using a self-consistent model.

2. Microwave Plasma Torch: Experiments and Simulation

Experiments were made with a microwave (MW) plasma generator with a MW power input up to 5 kW. This plasma torch is a part of an experimental set-up for treatment of inorganic salt solutions [11, 12]. A sketch of the MW plasma torch with the supposed flow patterns of gas and plasma is shown in Fig. 1.

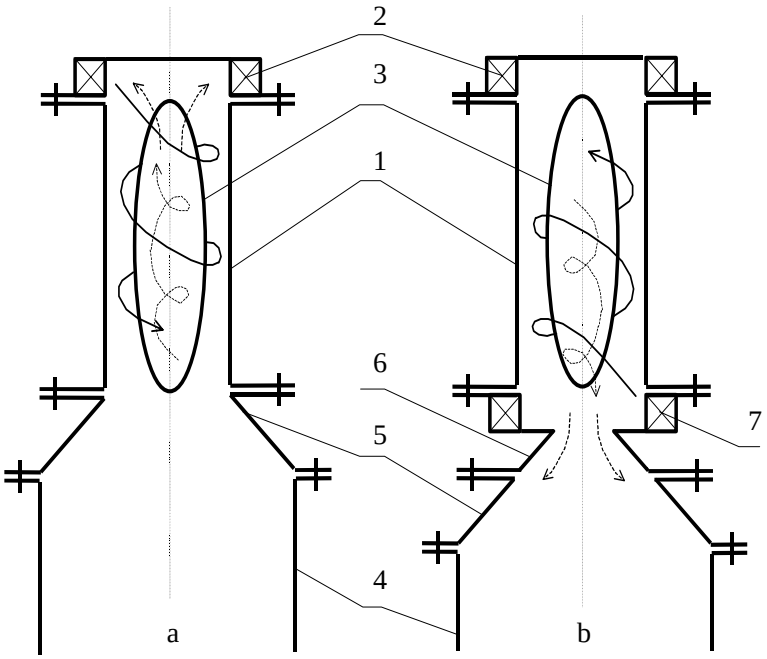

Fig. 1. Scheme of the MW plasma torches with supposed flow patterns of gas and plasma.
(a) – FVS scheme with flow patterns for conventional vortex plasma stabilization; (b) – RVS scheme with flow patterns for reverse vortex plasma stabilization.
1 - cylindrical quartz tube;
2 - original swirl generator;
3 - plasma;
4 - plasma chemical reactor;
5 - connecting cone;
6 - water-cooled diaphragm;
7 - additional swirl generator.

Calorimetric and electrical measurements permitted to determine the MW power input into the discharge (discharge power) and the heat losses to the water-cooled parts of the plasma torch. It was found that in experimental 3.5 kW power MW plasma torch with RVS the heat loses are 4-7 % of the discharge power depending on gas consumption. In the industrial MW plasma torch with FVS the heat loses are 26 - 42 %. Moreover, if the RVS is used, almost all the plasma forming gas should pass through the discharge zone. As the flow direction should be constant throughout the axial region, it seems possible to inject additional gas or particles into the "top" of the reverse vortex. Tests with ZrO_2+Y_2O_3 powder were made in the described MW facility. The introduction of the powder into the "top" of plasma torch with the RVS plasma ensures melting and spheroidization of particles up to 100 μm.

The numerical simulations of the MW plasma torch were made using the fluid flow and heat transfer simulation program FLUENT. In the 2D axisymmetric geometry the conservation equations for mass, energy and radial, axial and azimuthal momentum were solved simultaneously. To account for turbulence the Reynolds Stress Model (RSM) was used. Simulated flows are presented in Fig. 2. It is easy to see (Fig. 2b) that the reverse vortex "compresses" the hot zone and protects the plasma torch walls from overheating. As it was initially supposed [2], the main part of the plasma gas passes through the high temperature discharge zone and the size of recirculation zones are considerably reduced. In the FVS scheme (Fig. 2a), on the contrary, the main part of the incoming gas mixes with the hot recirculated flow and moves along the cylindrical quartz wall thus bypassing the discharge zone. A discrepancy between experimental and calculated results for heat loses was small

enough to conclude that the energy losses might be reliably predicted for MW electric discharges by employing numerical simulation models.

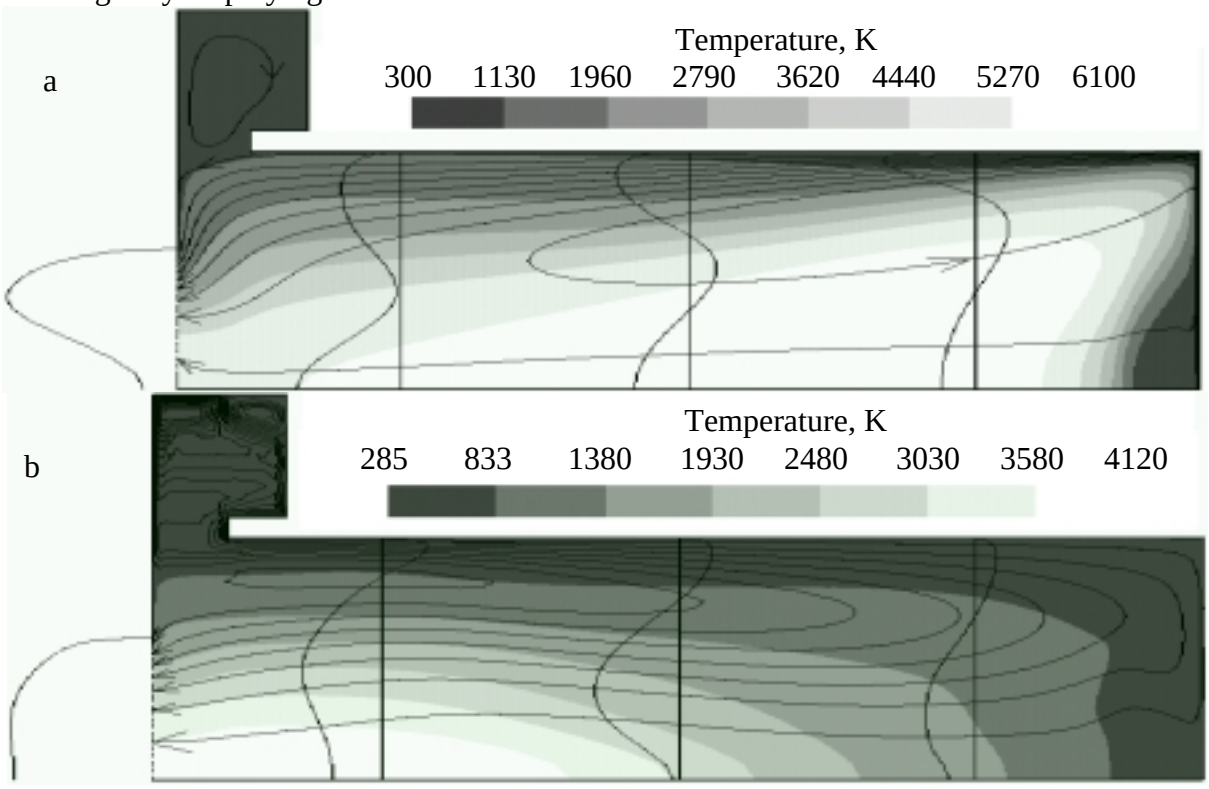

Fig. 2. Modelling results for MW plasma torch.
Temperature distribution, streamlines and profiles of axial velocity for three different cross-sections and for outlet of the MW plasma torches FVS (a) and with RVS (b).

3. Radio Frequency Inductively Coupled Plasma Torch: Experiments and Simulation

The scheme of the RF inductive plasma torch with the reverse vortex flow is shown on Fig. 3. Plasma gas enters the discharge volume through tangential swirler (2). The water-cooled nozzle (1) prevents immediate exit of the plasma gas from the volume. To compare the efficiencies of the RVS ICP and FVS ICP torches of the same geometry as plasma jet generators, total calorimetric measurements and numerical simulations were made using atmospheric pressure argon plasma. The FVS ICP torch geometry differs from the usually used one only by the nozzle ((1) on Fig. 3) on the plasma exit end.

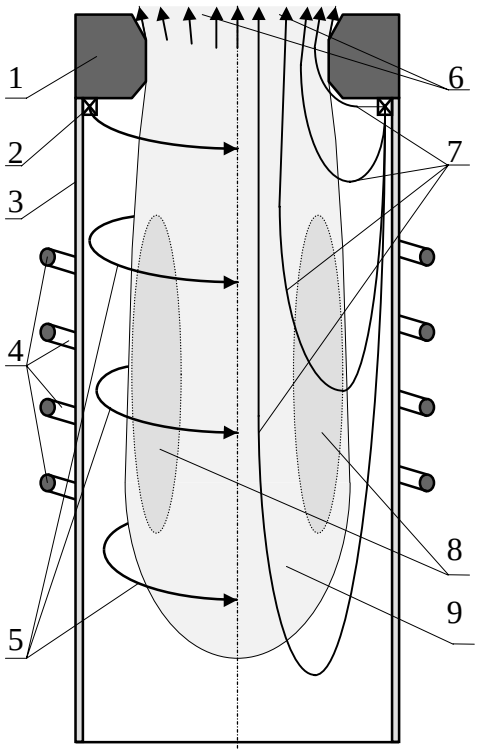

Fig. 3. Scheme of the inductively coupled RF plasma torch with RVS.
1 - water-cooled nozzle, 2 - tangential gas feeder, 3 - quartz tube, 4 - induction coil, 5 - gas streamlines, 6 - exit plasma flow, 7 - streamlines of the gas and plasma in the radial plane, 8 - skin layer, 9 - ICP.

The power characteristics of the FVS ICP, such as the dependence of the average plasma jet enthalpy on the plate power and the dependence of the plasma torch efficiency on the discharge power (Fig. 4) are typical. Here the plasma torch efficiency η is the ratio of the plasma jet power W_j to the total discharge power W_d: $\eta = W_j/W_d$. Plate power increase under a constant argon mass flow rate results in an increase of the average plasma jet enthalpy from 0.8 kJ/g to 3 kJ/g. Argon mass flow rate increase under a constant plate power results in a decrease of the average plasma jet enthalpy. The plasma torch efficiency drops with the growth of the discharge power and with the decrease of argon mass flow rate (Fig. 4). Thus, the FVS ICP is able to generate a high enthalpy plasma jet with low efficiency or a low enthalpy plasma jet with rather high efficiency. It is possible also to see in Fig. 4 that the simulation results are in a reasonable agreement with the experimental results. In this case the non-self-consistent approach was used [9] for simulation.

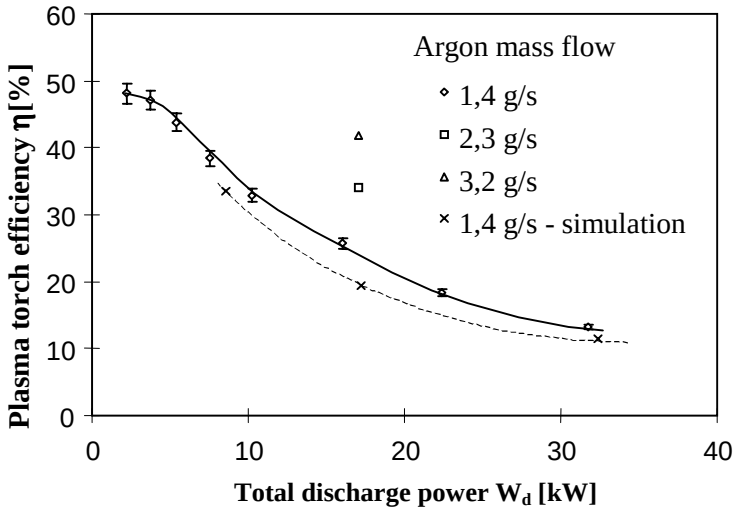

Fig. 4. Argon FVS ICP. Dependence of the plasma torch efficiency on the total discharge power for different argon mass flow. Experimental and simulation.

The plasma torch efficiency for the RVS (Fig. 5) also drops with the growth of the discharge power and the decrease of the gas flow rate, though η reaches a higher level than in the FVS ICP.

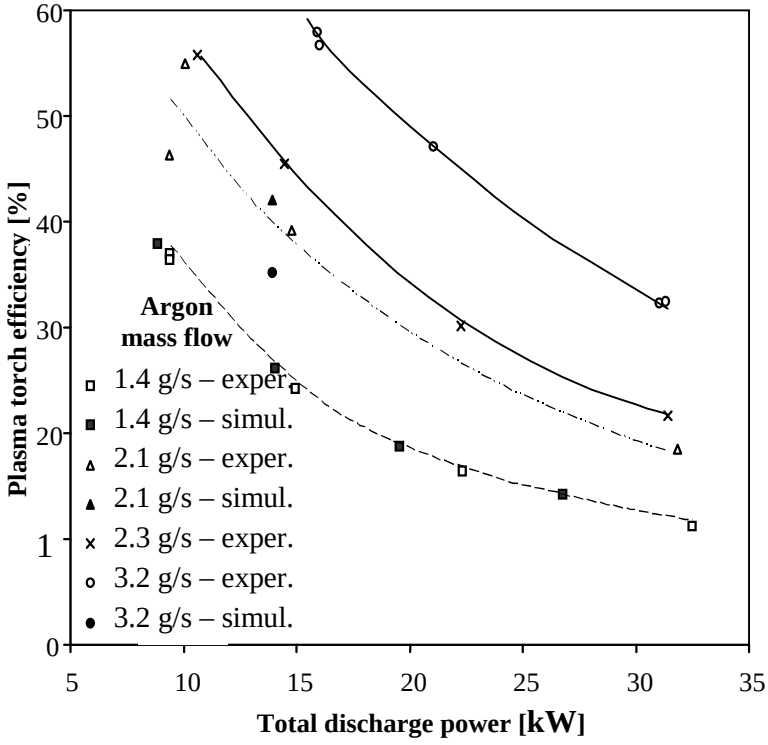

Fig. 5: Argon RVS ICP. Dependence of the plasma torch efficiency on the total discharge power for different argon mass flow. Experimental and simulation.

The average enthalpy of the argon plasma jet generated by the RVS ICP is higher than 2 kJ/g in all cases. It grows up to 3.2 kJ/g not only with the plate power increase, but also with increase of argon mass flow rate, and this is extremely unusual for any type of discharge. It means that the RVS ICP torch is capable

of generating a high enthalpy plasma jet with a high efficiency, which is very useful in various applications. Fig. 5 also shows that the modeling results even with the non-self-consistent approach [9] for the plasma jet generation efficiency of the RVS ICP torch was in good agreement with experiments. A large discrepancy between the experimental curve and the simulated result can be seen only beyond the experimentally observed range of discharge stability (see data for the argon mass flow 3.2 g/s and 14 kW power). Later numerical simulation was performed with the help of self-consistent model and the new results are qualitatively agreed with the previously obtained ones [9].

Replacement of FVS by RVS for argon ICP torch did not result in strong increase of heat efficiency due to high radiation and specific circular geometry of heat generation zone. Nevertheless the RVS ICP torch has some important advantageous in comparison with all traditional ICP torches – less gas consumption and possibility to inject an additional axial flow from the closed end of the system without substantially disrupting the flow pattern.

4. Experimental investigation of the gas burners

From the thermal insulation point of view a flame may be considered as low energy dense plasma. A comparative investigation was carried out for the experimental vortex gas burners with conventional FVS and with RVS. Schemes of the burners are presented in Fig. 6.

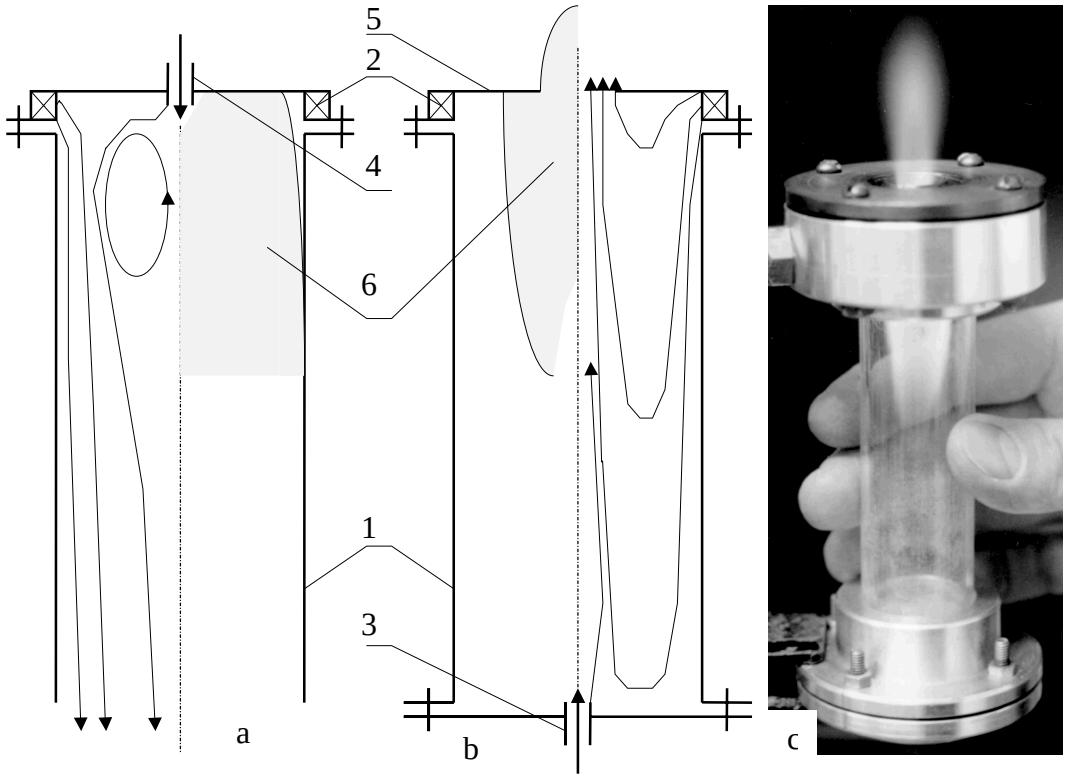

Fig. 6. Schemes and picture of the gas burners of 2 kW power.
(a) – with FVS; (b) and (c) – with RVS. 1 – quartz tube; 2 - tangential air feeder for swirl flow formation; 3 and 4 – fuel gas injection; 5 – diaphragm for flame jet exit.

Propane-butane mixture was used as a fuel and air as oxidant. In all experiments consumption of fuel gas and air was constant and calculated power of the burner was 1800 ± 300 Wt. Energetic characteristics of the burners were examined using gas temperature

measuring and calorimetric water-cooled tube which was connected with the outlet of burner or acted for the burner side wall. These characteristics are presented in Table 1 as gas temperature T_g and gas heat power W_g after calorimetric tube, calorimetric power W_c, total power W_Σ and concentration of nitrogen oxides C_{NO}.

Table 1. Energetic characteristics of the examined burners

Type of burner	W_c, Wt	T_g, K	W_g, Wt	W_Σ, Wt	C_{NO}, %
Reverse-vortex	1570±30	780±10	400±15	1970±40	0,35
Direct-vortex	1250±25	490±10	155±10	1405±30	0,41
Cooling direct vortex	1400±30	560±10	215±10	1615±35	0,46

The quartz wall of the conventional direct vortex burner was heated up to red glow while the reverse vortex burner may be handhold without any special cooling (Fig. 6c). So, heat loses to the wall of the reverse vortex burner cannot be more than 100 Wt.

5. Conclusion

Experimental investigations and numerical simulations show that RVS is very promising for different high temperature applications. A discrepancy between experimental and calculated results is small enough to conclude that the energy losses might be reliably predicted on the design stage of electrodeless plasma torches with the both types of vortex stabilization.

References

[1] A. F. Gutsol, Patent 2086812 RU, Izobreteniya (Inventions) (1997), No. 22, 344.
[2] V. T. Kalinnikov and A. F. Gutsol, Doklady Akademii Nauk, **353**, 469-471 (Physics - Doklady **42**, 179-181) (1997).
[3] J. W. McKelliget and N. El-Kaddah, J. Appl. Phys. **64** (1988), 2948 - 2954.
[4] A. Gutsol, J. Larjo, R. Hernberg, Proc. of ISPC 14, Prague, August 2-6, 1999, 227 – 231.
[5] V. T. Kalinnikov and A. F. Gutsol, Doklady Akademii Nauk, **360 (**1998), 49-52 (Physics - Doklady **43**, 302 - 305) (1998).
[6] A. F. Gutsol and V. T. Kalinnikov, Teplofizika vysokikh temperatur **37**, 194-201 (High temperature **37**, 172-179) (1999).
[7] A. Gutsol, Progress in Plasma Processing of Materials 1999, Begell House Inc., 81-86.
[8] A. Gutsol and J. A. Bakken, Proc. of ISPC 13, Beijing, Aug.18-22, 1997, 155-160.
[9] A. Gutsol and J. A. Bakken, J. Physics D: Applied Physics **31** (1998), 704-711.
[10] A. Gutsol, J. Larjo and R. Hernberg, Proc. of ISPC 14, Prague, August 2-6, 1999, 275 - 280.
[11] A. Gutsol and A. Agulyansky, Proc. of ISPC 10, Bochum, August 4-9, 1991, 1.4-15, 1-6.
[12] A. F. Gutsol, Khimiya Vysokikh Energiy (High Energy Chemistry), **29** (1995), 373-376 (Russ.), 344-347 (Eng.).